Effect of high power microwave injection on ozone balance

Cite as: AIP Advances **9**, 015221 (2019); https://doi.org/10.1063/1.5082522
Submitted: 21 November 2018 . Accepted: 07 January 2019 . Published Online: 23 January 2019

Yaogai Hu, Xiaoli Zhu, Lina Chen, and Zhengyu Zhao

Effect of high power microwave injection on ozone balance

Cite as: AIP Advances 9, 015221 (2019); doi: 10.1063/1.5082522
Submitted: 21 November 2018 • Accepted: 7 January 2019 •
Published Online: 23 January 2019

Yaogai Hu,[1,a)] Xiaoli Zhu,[1] Lina Chen,[2] and Zhengyu Zhao[1]

AFFILIATIONS

[1]Ionospheric Laboratory, School of Electronic Information, Wuhan University, Wuhan 430072, China
[2]Institute of Rock and Soil Mechanics, Chinese Academy of Sciences, Wuhan 430071, China

[a)]Author to whom correspondence should be addressed: yaogaihu@whu.edu.cn

ABSTRACT

High power microwave (HPM) injection into the troposphere to block the chain of chlorofluorocarbons (CFCs) or injection into the stratosphere to promote ozone generation are two feasible methods to artificially affect the ozone number concentration. Based on Maxwell's equations and current density control equations, this study adopts the finite difference time domain (FDTD) method to quantitatively analyze the process of HPM injection into different heights of atmosphere. By taking consideration of the main atmospheric components and the major chemical reactions in the atmospheric, the decomposition of CFCs and the change of the ozone number density is also quantitatively simulated in response to the injection of single pulse microwaves. The numerical simulation results show that under the injection of high power microwaves, the number density of electrons increased exponentially with time, reaching a maximum value of $10^{17}cm^{-3}$, and it increased considerably with the pulse time of injected high power microwaves and finally saturates when the state of atmospheric breakdown occurs. The decomposition of CFCs mainly occurs in the electron relaxation process, and the decomposition rate can reach 6% according to the simulation result. Before the atmosphere breaks down occurs, increase of microwave intensity or pulse width facilitates the production of more free electrons, which can consequently lead to a considerable increase in the ozone number density in ozone layer for a prolonged period.

I. INTRODUCTION

Ozone in nature is mainly derived from the three-body collision between oxygen atoms and oxygen molecules. With the strong ultraviolet rays at high altitudes, the oxygen molecules are largely dissociated, while the ultraviolet intensity at low altitudes is too low to generate enough oxygen atoms, so that the ozone layer mainly exists in the lower part of the stratosphere, about 30 to 50 km from the earth.

With the development of modern science and technology, the massive emission of chlorofluorocarbons (CFCs, also known as freon) and hydrobromofluorocarbon (HBFC) etc. posed a serious threat to the ozone layer. These substances are very stable in the atmosphere and are hardly decomposed by visible light, ozone, and free radicals like OH. Once they reach to ozone layer, CFC molecules will be decomposed under the action of solar UV radiation liberating atomic chlorine and chlorine-containing radicals, destroying the ozone in the following catalytic ways (for example, CFCs):

$$Cl + O_3 \rightarrow ClO + O_2,\ ClO + O \rightarrow Cl + O_2 \quad (1)$$

Usually one free radical of Cl can react with 10^5 O_3 molecules. That is to say, even a few amount of CFCs can decompose a large numbers of ozone molecules. To solve this problem, many scholars have proposed the methods of positively affecting the state of the atmosphere and improving the environment,[5] which can be roughly divided into two categories:

(1) Finding ways to remove atmospheric ozone-destroying substances;
(2) Generate artificial ozone source in the stratosphere to make up for ozone depletion.

As for the first method, Wong et al.[36] and Tsang et al.[33] proposed that microwaves should be used to convert the stratospheric Cl atoms into Cl anions (Cl^{-1}) which does not participate in the catalytic decomposition of the ozone. Stix[29] discussed the possibility of using strong laser to decompose tropospheric CFCs and found that when the radio power density is 1 MW/cm^2, the decomposition rate of CFCs can reach to 5.1×10^5/s. In the early 1990s, Askaryan et al.[3,4] proposed a scheme for decomposing CFCs in the troposphere (under 10 km) by generating a large amount of electrons by microwave discharge. Moreover, scholars like Kang and Wallis et al. also conducted experiments and analyzed the mechanism of decomposition of CFC-12 (CF_2Cl_2) in non-equilibrium plasma, obtaining a substantial decomposition efficiency of CFCs.[18,27,35] For the second type of method, create an artificial ozone source to compensates the O_3 loss in stratosphere by gas discharge is one of the most popular proposals aimed to restore the Earth's ozone layer.[28] The idea was first proposed by Gurevich et al.,[11] since then a series of experimental and theoretical works was conducted.[6,13,21,34] Vikharev et al.[34] theoretically discussed the possibility of regenerating ozone in the artificial ionization zone. Borisov et al.[6] has proposed a plasma-chemical model for the detailed investigation of the aeronomy of the atmosphere and lower ionosphere during microwave discharges. The steady growth of ozone is demonstrated for the electric field amplitude, pulse length and pulse repetition rate during microwave discharges.[2,6,14]

Microwave gas ionization has been extensively investigated for more than half a century.[22,26] Nowadays, some scholars devote themselves to the law of atmospheric propagation of high power microwave (HPM) pulse through the FDTD method.[30,39,42] FDTD method was found to have a good feasibility, validity and high computation efficiency in dealing with the issue of HPM atmospheric propagation.[38] A theoretical model of interactions between HPM and plasma was established,[15,39] and both variations of plasma density and transmission property of HPM were analyzed by FDTD method. Before conduct the experiment of HPM injection into the atmosphere to restore the ozone layer and clean the atmosphere, it is very necessary to carry out preliminary theoretical analysis and numerical simulations to provide theoretical support for the experiment. From the technical and economic point of view, the feasibility of producing an artificial ozone source in the stratosphere is open to question. Meanwhile, high-power microwave discharge also has a series of problems, such as the excessive power required, how to maintain the ionization state, and the problem of radio reflection in the artificial ionization region etc. These all will affect the possibility of microwave discharge in stratosphere to generate ozone.[1,5] Even so, most scholars hold a positive attitude toward chemical atmospheric purification of atmospheric by microwave discharge.

This paper is organized as follow. The chemical mechanisms that affect the ozone balance in the atmosphere by microwave injection are described in section II. Section III gives the atmospheric ionization model with high power microwaves, which is analyzed by FDTD method, and the ionization results under different microwave conditions is also given. Section IV is devoted to presenting the simulation results of CFCs decomposition and ozone generation. In addition, some discussion and analysis of the results are also given in this section.

II. PLASMA-CHEMICAL PROCESSES

A. Dissociation of CFCs in troposphere

During the ionization of microwaves to produce electrons, CFCs in steady state can be dissociated by collision with some of the electrons. It has been shown that dissociation by rapid electron bombardment is the most significant decomposition process,[5] but it is not the most effective one. Instead, the slow electron with a slower moving speed that dissociates by adhering to CFCs molecules to promote their decomposition is the main one. The dissociation process for slow electrons is as shown in (2) and (3):

$$CF_2Cl_2 + e \rightarrow Cl^- + CF_2Cl \tag{2}$$

$$CFCl_3 + e \rightarrow Cl^- + CFCl_2 \tag{3}$$

$CFCl_3$ (CFC-11) and CF_2Cl_2 (CFC-12) are very "brittle" (easily decomposed) during interaction with slow electrons. The reaction coefficients for (2) and (3) are:[4]

$$\begin{cases} \left.\begin{aligned} k_D^{(CFC-12)} &= \left\langle \sigma_D^{CFC-12} v_e \right\rangle \approx 2.05 \times 10^{-9}\ cm^3 s^{-1} \\ k_D^{(CFC-11)} &= \left\langle \sigma_D^{CFC-11} v_e \right\rangle \approx 8.86 \times 10^{-8}\ cm^3 s^{-1} \end{aligned}\right\} T_e \approx 0.02707 eV (240K) \\ \left.\begin{aligned} k_D^{(CFC-12)} &\approx 1.85 \times 10^{-9}\ cm^3 s^{-1} \\ k_D^{(CFC-11)} &\approx 2.87 \times 10^{-8}\ cm^3 s^{-1} \end{aligned}\right\} T_e \approx 0.25 eV \end{cases}, \tag{4}$$

where $k_D^{(CFC-12)}$, $k_D^{(CFC-11)}$ is the reaction coefficient of (2) and (3) respectively. The electron temperature in (4) is relatively low, but the two reaction constants are large, which because a low electron temperature means that the electron energy is also low, but the reaction coefficient can be so large because the affinity between the electron and the chlorine atom is much greater than the dissociation energy of the CFCs molecule. At the same time, it is also found that the reaction

coefficient k_D corresponding to the higher electron temperature T_e is smaller. In addition to the chemical processes described above for the direct breakdown of CFCs, there are also chemical processes[4] that indirectly decompose CFCs. The efficiency of these processes are not competitive with CFCs as they are with cold plasma electrons. Therefore, this paper neglects the effects of other processes, and consider the dissociation and attachment reaction as the main process of decomposing CFCs during microwave discharge.

Knowing the reaction coefficient of the chemical reaction process and the initial number density of particles, the relationship between the number density of particles and time can be calculated according to the chemical reaction theory. In addition to calculating the effect of changing electron density on the decomposition of CFCs by chemical reaction theory, scholars[4] also gave a rough calculation of the efficiency formula of CFCs decomposition. Under the assumption that the electron density is far greater than the number density of CFCs (i.e., $N_e \gg n_{CFC0}$) during the interval of microwave pulses, where N_e is the electron number density and n_{CFC0} is the number density of CFCs, and that the dissociation mechanism of free electrons on CFCs mainly depends on the attachment dissociation reaction, approximate solution of the relative amount of decomposition of CFCs in the electronic dissociation is as following:

$$\eta_{CFC0} \approx 1 - (1 + \alpha_r N_e t)^{-\gamma} \tag{5}$$

where $\eta_{CFC0} \equiv \Delta n_{CFC}/n_{CFC0}$, $\Delta n_{CFC} = n_{CFC0} - n_{CFC}(t)$, and $n_{CFC}(t)$ is the is number density of CFCs molecule at time t, n_{CFC0} is the initial number density of CFCs. $\gamma = k_D^{CFC}/\alpha_r$, where α_r is the composite coefficient of free electrons and positive ions, k_D^{CFC} is the reaction coefficient. It is obvious that the relative amount of CFCs to be decomposed by electron attachment dissociation is proportional to the free electron density N_e and the dissociation adhesion constant k_D^{CFC}. That is to say, the greater the electron number density and the reaction constant, the greater the CFCs decomposition rate.

B. Promote ozone generation in stratosphere

The injection into ozone layer by HPM can lead to an increase in the number density of gas particles in the active region, which involved in a lot of chemical reactions. Ouyang et.al.[25] proposed that 32 particles participated in 166 reactions during the microwave pulse, but these are still incomplete. Here we will simplify the chemical mechanism of ozone homeostasis and focus on the discussion of major particles and chemical reactions that can affect ozone production. The results of previous studies show that the increase free electrons in the atmosphere facilitates the conversion of O_2 into O_3, which will eventually increase the number density of ozone.

The first stage of the process of ozone generation by microwave injection is the production of atomic oxygen. The dissociation by electron impact will be responsible for oxygen atom production[14] (all the reaction rate constant of chemical reactions below can be found in Table I)

TABLE I. The major chemical reactions during microwave injection.

Reaction process	reaction rate
$O_2+e \rightarrow 2O+e$	$4.2\times10^{-9}\exp(-5.6/T_e)$ cm^3/s
$N_2+e \rightarrow N_2(A^3\sum_u^+)+e$	10^{-12} cm^3/s
$N_2+e \rightarrow N_2(B^3\prod_g)+e$	10^{-9} cm^3/s
$O_2+N_2(A^3\sum_u^+) \rightarrow 2O+N_2$	2×10^{-12} cm^3/s
$O_2+N_2(B^3\prod_g) \rightarrow 2O+N_2$	3×10^{-10} cm^3/s
$O+N_2(A^3\sum_u^+) \rightarrow O+N_2$	10^{-11} cm^3/s
$N_2^*+O \rightarrow NO+N$	6.5×10^{-12} cm^3/s
$O+O_2+N_2 \rightarrow O_3+N_2$	$6.2\times10^{-34}\exp(300/T)^2$ cm^6/s
$O+O_2+O_2 \rightarrow O_3+O_2$	$6.9\times10^{-34}\exp(300/T)^{1.5}$ cm^6/s
$O+O+N_2 \rightarrow O_2+N_2$	$3\times10^{-33}\exp(300/T)^{2.9}$ cm^6/s
$O+O+O_2 \rightarrow 2O_2$	6.7×10^{-33} cm^6/s
$O+O_3 \rightarrow 2O_2$	$1.8\times10^{-11}\exp(-2300/T)$ cm^3/s
$NO+O_3 \rightarrow NO_2+O_2$	$4.3\times10^{-12}\exp(-1560/T)$ cm^3/s
$NO_2+O \rightarrow NO+O_2$	$1.8\times10^{-12}\exp(-120/T)$ cm^3/s
$N+O_2 \rightarrow NO+O$	$4.4\times10^{-12}\exp(-3220/T)$ cm^3/s
$NO+N \rightarrow N_2+O$	$1.05\times10^{-12}T^{0.5}$ cm^3/s

$$O_2 + e \rightarrow 2O + e \tag{6}$$

where T_e is the electron temperature (K) which is mainly determined by the electric field strength during the pulse[8]

$$\begin{cases} T_e = 0.4 \times (\frac{E_e}{p})^{0.577}, 30 \le \frac{E_e}{p} < 54 \\ T_e = 2.17 \times (\frac{E_e}{p})^{0.15}, 54 \le \frac{E_e}{p} < 120 \\ T_e = 0.18 \times (\frac{E_e}{p})^{0.65}, 120 \le \frac{E_e}{p} \le 3000 \end{cases} \tag{7}$$

where T_e is in eV; p is the air pressure in torr. Besides, electron-excited nitrogen molecules N_2^* (considering chiefly $N_2(A^3\sum_u^+)$ and $N_2(B^3\prod_g)$) are produced by electron impact[9,11,23]

$$N_2 + e \rightarrow N_2^* + e \tag{8}$$

The interaction with oxygen molecules can produce oxygen atom

$$O_2 + N_2^* \rightarrow 2O + N_2 \tag{9}$$

Along with process (9), there are quenching reaction upon their collisions with molecules

$$O + N_2(A^3\sum_u^+) \rightarrow O + N_2 \tag{10}$$

$$N_2^* + O \rightarrow NO + N \tag{11}$$

The above discussed kinetic processes are responsible for atomic oxygen production. At the second stage, the produced atomic oxygen undergoes a three-body recombination reaction with O_2, producing O_3[10]

$$O + O_2 + M \rightarrow O_3 + M \tag{12}$$

The remainder of oxygen atoms will again bond to form oxygen molecules

$$O + O + M \rightarrow O_2 + M \tag{13}$$

Meanwhile, the oxygen atoms are involved in a relatively slow ozone decomposition reaction

$$O + O_3 \rightarrow 2O_2 \tag{14}$$

Moreover, it should be noted that the change in the UV transparency of air in ozone depletion area will also affect the photochemical process in this area. The destruction of ozone results in bleaching of the atmosphere in the UV range, which produces a negative feedback that restores the ozone.[19,20] The process of the photodissociation of O2 will be promoted by the hard UV radiation, so that Oxygen atoms are formed, and then these atoms form ozone in the three-body recombination reaction (12). However, as we maintained the equilibrium of atmosphere by taking the reverse reactions into account, the role of the natural photolysis process is always balanced with the effects of other processes in the background, so the natural photolysis process is ignored in this paper.

In addition to the main reactions related to oxygen, we take minor constituents of the atmosphere into consideration. The reactions are shown below

$$NO + O_3 \rightarrow NO_2 + O_2 \tag{15}$$

$$NO_2 + O \rightarrow NO + O_2 \tag{16}$$

$$N + O_2 \rightarrow NO + O \tag{17}$$

$$NO + N \rightarrow N_2 + O \tag{18}$$

The major chemical reactions during microwave injection are summarized in Table I, where T is the atmospheric temperature in K which is correlated with altitude:

$$T = \begin{cases} 288.15 - 6.5h & 0 \le h \le 11\text{km} \\ 216.65 & 11 < h \le 20\text{km} \\ 216.65 + (h - 20) & 20 < h \le 32\text{km} \\ 228.49 + 2.64(h - 32) & 32 < h \le 48\text{km} \\ 270.65 & 48 < h \le 52\text{km} \\ 270.65 - 1.9(h - 52) & 52 < h \le 62\text{km} \\ 251.05 - 3.9(h - 62) & 62 < h \le 80\text{km} \\ 180.65 & 80 < h \le 90\text{km} \end{cases} \tag{19}$$

So many processes and components are involved in ozone generation during and after the microwave pulse, including excited state of oxygen molecules, atoms, positive ions, hydronium ions, electrons and so on.[24] But we will just consider the reactions mentioned above. Note that the atmosphere is in dynamic equilibrium state before the microwave injection. It will be non-equilibrium after the pulses if we only consider the positive reaction of above equations. Therefore, the reverse reactions are taken into consideration. The reverse coefficients can be obtained according to the initial number of particles and positive coefficients. Take formula (20) for example.

$$\frac{d[O]}{dt} = \bar{k}[O_3][N_2] - k[O][O_2][N_2] = 0 \tag{20}$$

where k is the reaction rate constant of reaction (12), $\bar{k}$ is the reverse coefficient.

III. ANALYSIS OF MICROWAVE ATMOSPHERIC PROPAGATION BY FDTD METHOD

A. Atmospheric propagation model of HPM

The atmospheric propagation model for HPM can be described by Maxwell's equations, current density control equations, electron density equations, and electron energy equations. FDTD[38] is used to convert Maxwell's equation into a set of difference equations. Based on the initial value and boundary conditions, the electromagnetic field distribution can be obtained step by step in time and space. The one-dimensional model is used as an example to describe the atmospheric propagation of HPM.[31] For the electromagnetic wave propagating in the z-direction, the electric field only has the x-direction component, the magnetic field only has the y-direction component, and the current density only has the x-direction component, the equations are as follows:[5,32,41]

$$H_y^{n+1/2}(k+1/2) = H_y^{n-1/2}(k+1/2) - \frac{\Delta t}{\mu_0 \Delta z} \times [E_x^n(k+1) - E_x^n(k)] \tag{21}$$

$$E_x^{n+1}(k) = E_x^n(k) - \frac{\Delta t}{\varepsilon_0 \Delta z}\left[H_y^{n+1/2}(k+1/2) - H_y^{n+1/2}(k-1/2)\right] - \frac{e\Delta t}{2\varepsilon_0}\left(U_x^{n+1/2}(k+1/2) + U_x^{n+1/2}(k-1/2)\right) \tag{22}$$

$$U_x^{n+1/2}(k+1/2) = \frac{e\Delta t}{4m}(E_x^n(k+1) + E_x^n(k))(n_e^n(k+1) + n_e^n(k)) + (1 - v_m\Delta t)U_x^{n-1/2}(k+1/2) \tag{23}$$

$$n_e^{n+1} = (1 + (v_i - v_a)\Delta t)n_e^n - \frac{\Delta t}{2\Delta z} \times \left(U_x^{n+1/2}(k+1/2) - U_x^{n+1/2}(k-1/2)\right) \tag{24}$$

where equations (21) and (22) are Maxwell equations; equation (23) is the current density governing equation; and equation (24) is the electron density equation. E_x, H_y, ε_0 and μ_0 is the electric field strength in the x direction, the magnetic field strength in the y direction, the permittivity and the permeability of the free space respectively. U_x is the component current density along the x direction of the electron fluid velocity; n_e is the electron density, $e = -1.6 \times 10^{-19}$ C is the electron charge, $m = 9.3 \times 10^{-31}$ kg is the electron mass; v_m, v_i, v_a, v_ω is collision frequency of electrons and neutrals, ionization frequency, adhesion frequency and energy transfer rate respectively. Using the initial value and the boundary conditions to iteratively solve the equations (21) ~ (24), the ionization of HPM into the atmosphere can be obtained.

While HPM pulse injection, the electron density increases sharply and will be in an unbalanced state. After stopping the pulse, the electron density without an excitation source will decrease and then gradually return to the equilibrium state from the non-equilibrium state, which called the electronic relaxation process. During the pulse interval, the recombination and attachment effects of free electrons are the main factors affecting the electronic relaxation process. The effect of electron diffusion is negligible,[17] and the electron density in the relaxation process can be calculated by the following formula calculation:

$$\frac{\partial N_e}{\partial t} = -\nu_r N_e - \nu_a N_e \tag{25}$$

where υ_r is the electronic compound frequency, υ_a is the frequency of electronic attachment. The solution is:

$$N_e = \frac{N_{e0}\nu_a}{(\nu_a + \upsilon_r)e^{\nu_a t} - \nu_r} \tag{26}$$

where N_{e0} is the initial electronic density of the electron relaxation process, that is, the electron density at the very end of the microwave pulse. During the pulse interval, after removing the microwave electric field, the attachment frequency υ_a and the composite frequency υ_r are related to the atmospheric pressure p and the electron temperature T_e[12,37] as shown in (27) to (29):

$$\upsilon_r = N_e\left(4.8T_e^{-0.39} + 2.1T_e^{-0.63}\right) \times 10^{-14} \tag{27}$$

$$\upsilon_r = N_e\left(4.8T_e^{-0.39} + 2.1T_e^{-0.63}\right) \times 10^{-14} \tag{28}$$

$$T_e = \begin{cases} \dfrac{T_{e0} - T}{\left(1 + 0.98 \times 10^{-16} N_n t\sqrt{T_{e0} - T}\right)^2} + T, & T_{e0} > 1eV \\ \dfrac{T}{1 + (T/T_{e0} - 1)\exp\left(-1.96 \times 10^{-16} N_n Tt\right)}, & T_{e0} < 1eV \end{cases} \tag{29}$$

where T_{e0} is the electron temperature at t=0; T is the atmospheric temperature; and N_n is the density of neutral molecular numbers in the atmosphere.

B. FDTD numerical results

Using the initial value and the boundary conditions to iteratively solve the equations (21) ~ (24), the ionization of high power microwave into the atmosphere can be obtained. The initial value of the electric field component is the microwave electric field strength value, the initial value of the magnetic field component and the current density component is zero, and the initial value of electron number density is the free electron number density N_0. For the truncated boundary, one-dimensional absorption boundary conditions[10] are used in the electric field, and the hydromechanics boundary is applied to the number density of free electrons and current.[41] The initial number density of free electrons N_0 fits the empirical formula in different heights:[30]

$$N_0 = \begin{cases} 10 & h < 25\text{km} \\ 8 \times 10^7 \times (h/60)^{18} & h \geq 25\text{km} \end{cases} \tag{30}$$

The ozone balance that the article concerns is related with the amount of free electrons generated by microwave injection. Taking microwave injection in stratosphere as an example, the atmospheric ionization results under different microwave conditions are given below. The formation of free electrons or the characteristic of air breakdown in different stratospheric height s is analyzed under the same microwave pulse. For more details of microwave discharge excitation in specific region of the atmosphere you can see Askaryan et.al.[4] Here we only select typical ozone layer altitude 20 km, 25 km, 30 km and 35 km as the simulation parameters. The results of 40 km and 50 km are also presented as a contrast.

As can be seen from Figure 1a and Figure 1b, the waveform of microwave at 20 km and 25 km did not change obviously, and the electric field intensity did not attenuate obviously, which means no atmospheric breakdown occurred. However, from Figure 1c and Figure 1d, we can see that electric field intensity decayed considerably, there is the phenomenon of atmospheric breakdown. The time of atmospheric breakdown at 30 km, 35km, 40km and 50km was 4.9ns, 2.5ns, 2.2ns and 6.2ns respectively, corresponding to the maximum electron density values were 2.86×10^{16} cm^{-3}, 1.86×10^{16} cm^{-3}, 1.94×10^{16} cm^{-3}, 3.15×10^{16} cm^{-3}. From the breakdown time, it can be found that with the increase of altitude, the difficulty of air breakdown decreases and then increases. There is an extreme height between 35 km and 40 km, which is consistent with Zhao et al[40] The main reasons are as follows: In the lower atmosphere, the low concentration of free electron, dense air, high air pressure and other factors lead to a large degree of difficulty of ionization, however, as the height increases, the free electron density increases, the air becomes thinner, the pressure decreases and the air ionization becomes relatively easier, which means the difficulty of ionization will be reduced. After reaching a certain height (about 35km~40km), the electron density becomes larger, but more rarefied air leads free path of electrons become larger so that the difficulty of impact ionization increases. For free electrons generated by HPM injection, the maximum can be increased till atmospheric breakdown occurs, as shown in Figure 1c ~ 1f.

Assuming that the initial electron density in the relaxation process $N_{e0} = 10^{18}$ m^{-3}, and the initial electron temperature T_e = 16 eV, the relationship between electron number density and electron temperature vs. time during relaxation process can be obtained from Eqs. (26)~(29):

It can be seen from Figure 2 that during the relaxation process, as the height increases, the electron number density decreases more slowly, and it takes longer for electron temperature drops to the background atmospheric temperature. Comparing Figure 2a with Figure 2b, we can see that the time electron temperature declines much shorter than the decay time of electron number density during electronic relaxation process, that is, the electron temperature drops faster than the electron number density, and at different heights, the electronic relaxation process will be different, and the decrease rate of electron temperature and electron number density will decrease as the height increases.

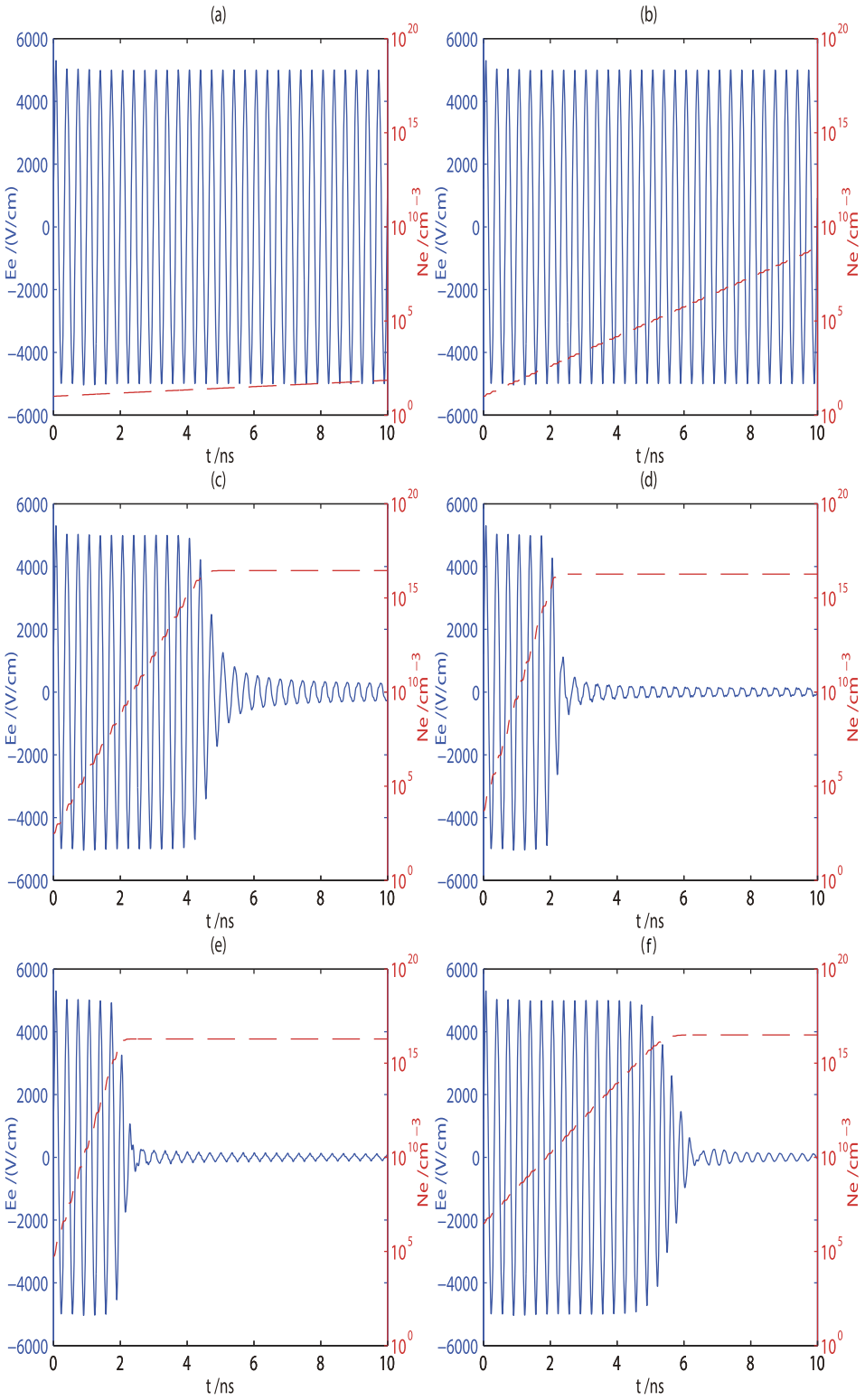

FIG. 1. Electron density (Ne) and electric field intensity (Ee) changes with time at different heights: (a)20km; (b)25km; (c)30km; (d)35km; (e)40km; (f)50km. Assumes that the waveform of HPM have no obvious change from the ground to the set altitude, and the incident wave propagates along the z-axis (vertical direction) with a center frequency of 3 GHz and a pulse width of 10ns, the electric field strength Ee is 4.8 kV/cm.

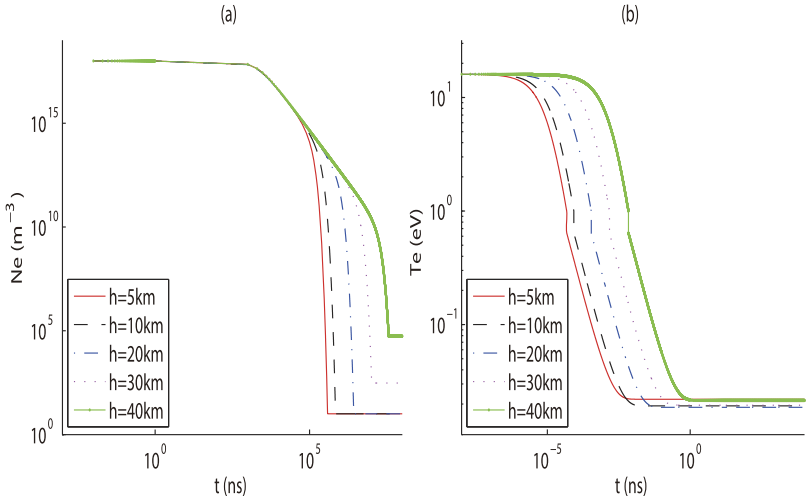

FIG. 2. Relation curves of the electron temperature and number density vs. time at different height in the relaxation process: (a) number density of electron; (b) electron temperature.

IV. NUMERICAL SIMULATION RESULTS AND DISCUSSION

A. Simulation results of tropospheric CFCs decomposition

The main substances contained in CFCs are CFC-11 and CFC-12, whose molecular densities are obtained from CDIAC (Carbon Dioxide Information Analysis Center). At a height of 3.58 km, [CFC-11] =1.03×10^{12} cm^{-3} and [CFC-12] =2.60×10^{12} cm^{-3}. Figure 3 shows the decomposition of CFCs under single-pulse microwaves at different field strengths, where the injection height, frequency and pulse width of microwave source are 3.58 km, 3 GHz, and 10 ns, and the entire calculation time is 1us. The final decomposition data of CFCs are shown in Table II.

As can be seen in Figure 3a, although the electron number density increased significantly, reaching to a maximum value of 4.15×10^{12} cm^{-3}, the number density of CFCs did not change significantly, and the decomposition efficiency was very low. Compared Figure 3b ~ 3d with Figure 3a, the electron density has reached the maximum value under the microwave pulse injection. The number density of CFCs obviously decreased after the injection, and as the field intensity increase, the more the amount of CFCs was decomposed, the higher the decomposition efficiency will obtain. At the same time, Figure 3b~3d also indicate that the amount of CFCs began to decline after the electron density reached a maximum value for a period of time. That's because the electron temperature is higher under the influence of the pulse so that the reaction coefficient of CFCs decomposition is small at this time, that's why although the electron has reached the number density that can promote the decomposition of CFCs during the pulse period, the amount of CFCs remains unchanged. However, after the injection of the pulse, the electron temperature starts to decrease and the reaction coefficients of (2) and (3) begin to increase, resulting in the rapid decomposition of CFCs. It can be seen from Table II that when the electron number density reaches 10^{17} cm^{-3}, the CFCs breakdown rate η_{CFC} will exceed 6%.

The decomposition efficiency of CFCs at 3.58 km under different microwave conditions is shown in Figure 4, where subgraph (a) shows the relationship between the decomposition rate of CFCs and the electric field intensity, while subgraph (b) shows the relationship between the decomposition rate of CFCs and the microwave frequency. As can be seen from Figure 4a, the decomposition rate of CFCs increases with the increase of electric field intensity, approaching to a maximum value. The reason is that although the time required to maintain the maximum number density of free electrons increases with the increase of the field intensity, under the effect of an electric field, the electron temperature is relatively high and the reaction coefficient of CFCs decomposition is small, so that the effect of CFC decomposition does not become obvious with the increase of the sustaining time. As shown in Figure 4a, the decomposition rate of CFCs at 70 kV/cm is about 8%. With the increase of microwave frequency, the decomposition rate of CFCs also almost linearly increased, and the decomposition rate of CFCs under microwave at 8 GHz is about 16%.

If we use the data given by the CDIAC data center as the initial CFCs concentration for all heights of the troposphere, then we can roughly get the CFCs decomposition rates for microwave pulses of different heights. As shown in Figure 5, the microwave injection at the altitude above 1km can effectively promote the decomposition of CFCs, and the decomposition rate rose slightly within 3~10 km, then declined, the decomposition rate is 8% to 10%. For the initial CFCs densities at all heights are the same, and microwave parameters are the same, the reason for different decomposition rates at different height is the difference in atmospheric environmental parameters, i.e., atmospheric temperature and atmospheric pressure slightly affect the decomposition of CFCs.

B. Formation efficiency of ozone in stratospheric

The initial number density of oxygen and nitrogen molecules can be calculated by the data of U.S Standard

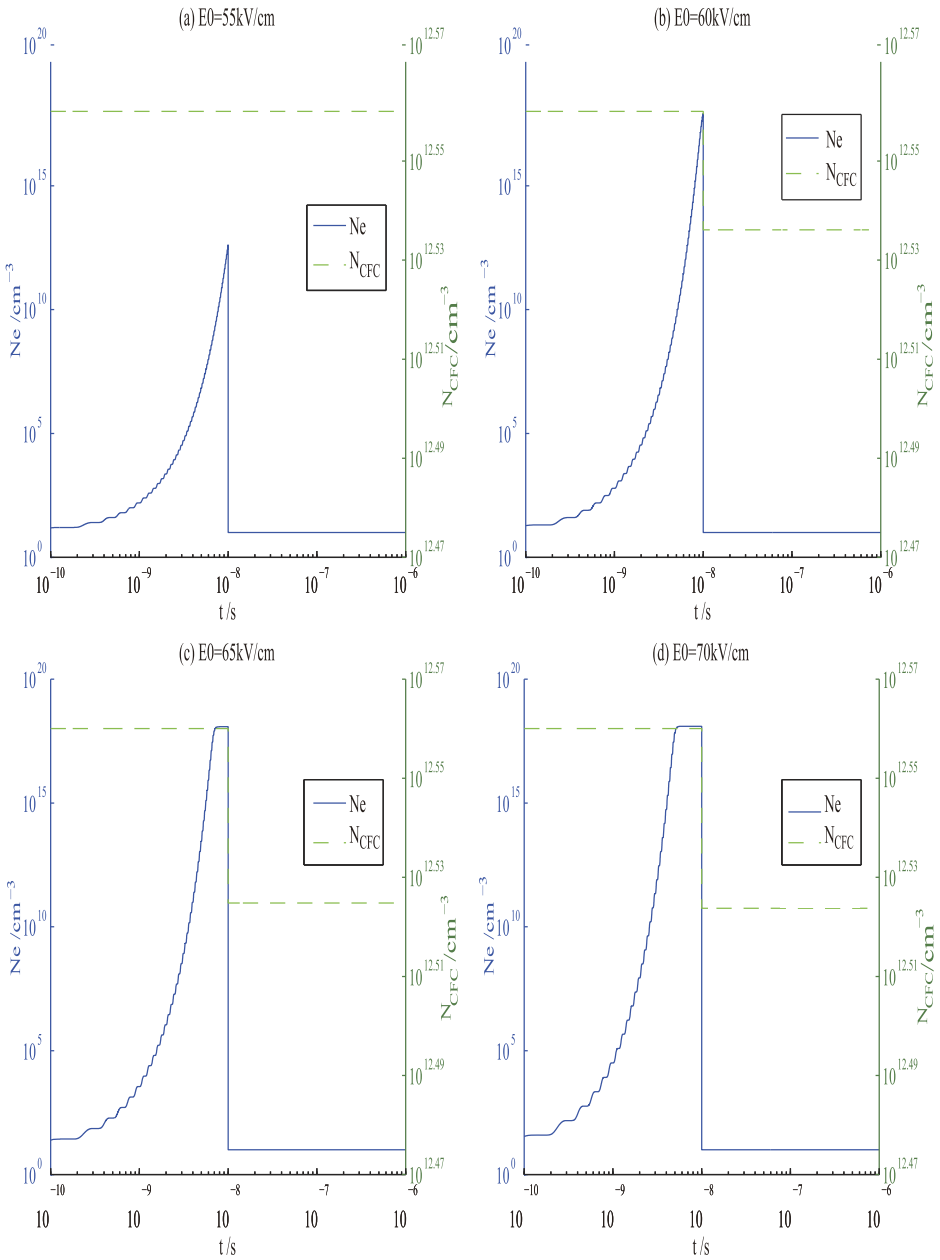

FIG. 3. CFCs' and electron number density vs. time at different electric filed intensity: (a) Am=55 kV/cm; (b) Am=60 kV/cm; (c) Am=65 kV/cm; (d) Am=70 kV/cm.

TABLE II. The Data of CFCs at Different Electric Field Intensity. Am is the microwave electric field intensity, Ne (max) is the maximum electron density achieved at the end of the microwave injection, ΔCFCs is the number density of CFCs decomposed in total in 1us, and η_{CFC} is the percentage decomposition of CFCs.

Am/V·cm^{-1}	55000	60000	65000	70000
Ne(max)/cm^{-3}	4.15×10^{12}	6.67×10^{17}	9.27×10^{17}	9.56×10^{17}
ΔCFCs/cm^{-3}	1.1154×10^{6}	1.6636×10^{11}	2.2446×10^{11}	2.3064×10^{11}
η_{CFC}	0	4.5818%	6.1812%	6.3521%

Atmosphere, 1976; and the initial number density of ozone, nitric oxide and nitrogen dioxide can be obtained by HALOE (Halogen Occultation Experiment) data, which is shown in Table III.[7,16,24]

The electron number density and the number of related particles with time during high-power microwave implantation can be obtained by simultaneous of equations (21) ~ (24) and the chemical reactions mentioned in section II. Figure 6 illustrates the changes of the number density of electrons, O, O_2, O_3, NO, NO_2 over time at different heights (20 km~35 km).

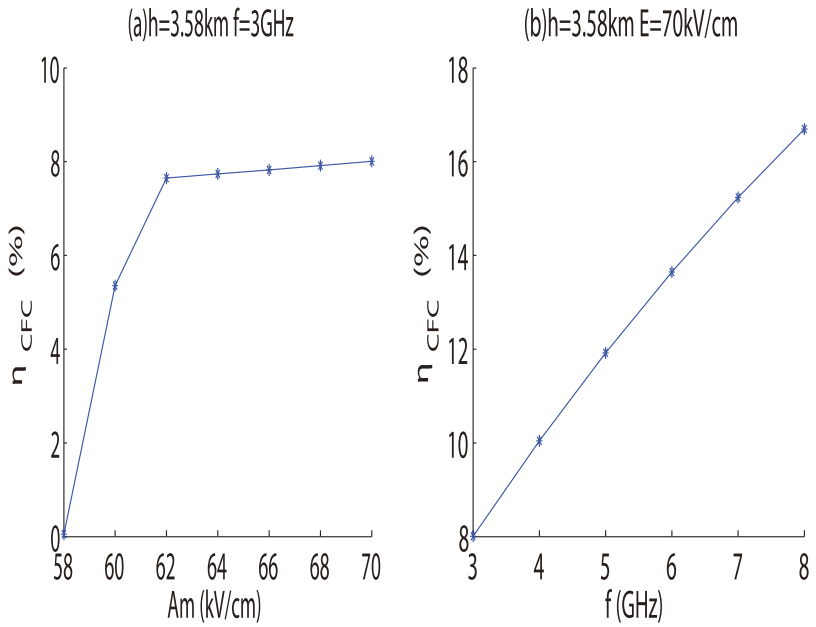

FIG. 4. The decomposition efficiency of CFCs, at different electric field intensity and frequency: (a) different electric field intensity, (b) different frequency.

The frequency, pulse width and intensity of microwave source are f=3 GHz, tp=10 ns and Ee=4.8 kV/cm.

Figure 6a and Figure 6b illustrate that, there is no obvious change in the ozone density at 20 km and 25 km. The densities of ozone at 30 km and 35 km shown in Figure 6c and Figure 6d compared with the initial number density increased by four orders of magnitude and maintained for about 400s. Comparing Figure 6 and Figure 1, we can see that the electron number density grows slightly at 20 km. And it grows significantly at the altitude of 25 km and promotes the generation of oxygen atoms but there's still no change in the number density of ozone. Apparently, the air breakdown and tail-erosion appears at the end of the pulse in Figure 1c~1d. Figure 6c~6d have similar results. When the electron number becomes appreciable, the number density of atomic oxygen and nitric oxide increase and oxygen decreases in reaction (6), (8), (9) and (11). After the electron number returns to the natural state, oxygen atoms achieve a high density of magnitude. It will promote the reactions (13) and (14) contributing the increase of oxygen molecules. While the number density of O_2 is big enough, the reaction (12) becomes the main source of ozone production and ozone number density begins to increase. The ozone number density can have a considerable increase and maintain for a period time. However, it will go down due to the reaction (14) and (15). As the Figure 6c shows, the maximum density of O_3 is about 1.02×10^{16} cm^{-3} and O_2 is 5.87×10^{16} cm^{-3} in the meantime. $[O_3]$ has four orders of magnitude greater than the initial time and $[O_2]$ reduces 1.53×10^{16} cm^{-3}. Most reduction of oxygen is used to synthesize ozone. In the Figure 6d, $[O_3]$ is about 3.07×10^{15} cm^{-3} at the maintaining state and goes up by three orders of magnitude.

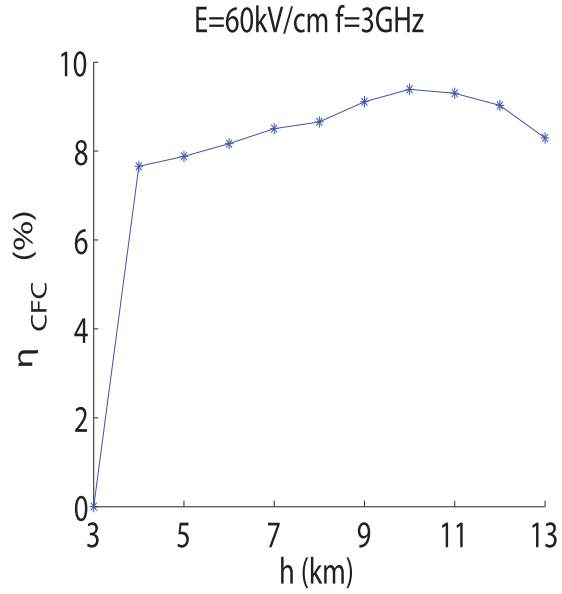

FIG. 5. The decomposition efficiency of CFCs at different height.

The analysis shows that HPM can facilitate the formation of ozone in ozone layer (20-35 km), and remain for a considerable time (the $[O_3]$ can stay high about 100 seconds and it will cost at least 10^5 seconds to return to natural state) but different altitudes correspond to different promoting effects. We select the height 30 km where is the place a higher ozone concentration and easier to produce electrons to analyze the effect of different pulse field strength and pulse width on ozone balance. Figure 7 presents the time dependence of the number density of electrons, O, O_2, O_3, NO, NO_2 for f=3 GHz

TABLE III. The Initial Number Density of O, O_2, O_3 and Other Particles in Different Atmospheric Height.

Height/km	$[O]/cm^{-3}$	$[O_2]/cm^{-3}$	$[O_3]/cm^{-3}$	$[N_2]/cm^{-3}$	$[NO]/cm^{-3}$	$[NO_2]/cm^{-3}$
20	1.0×10^{6}	3.6×10^{17}	2.9×10^{12}	1.4×10^{18}	2.6×10^{7}	3.4×10^{8}
25	7.0×10^{6}	1.6×10^{17}	4.1×10^{12}	6.6×10^{17}	2.1×10^{8}	9.6×10^{8}
30	4.0×10^{7}	7.4×10^{16}	2.6×10^{12}	2.9×10^{17}	6.5×10^{8}	1.3×10^{9}
35	2.0×10^{8}	3.5×10^{16}	1.3×10^{12}	1.3×10^{17}	7.4×10^{8}	5.8×10^{8}

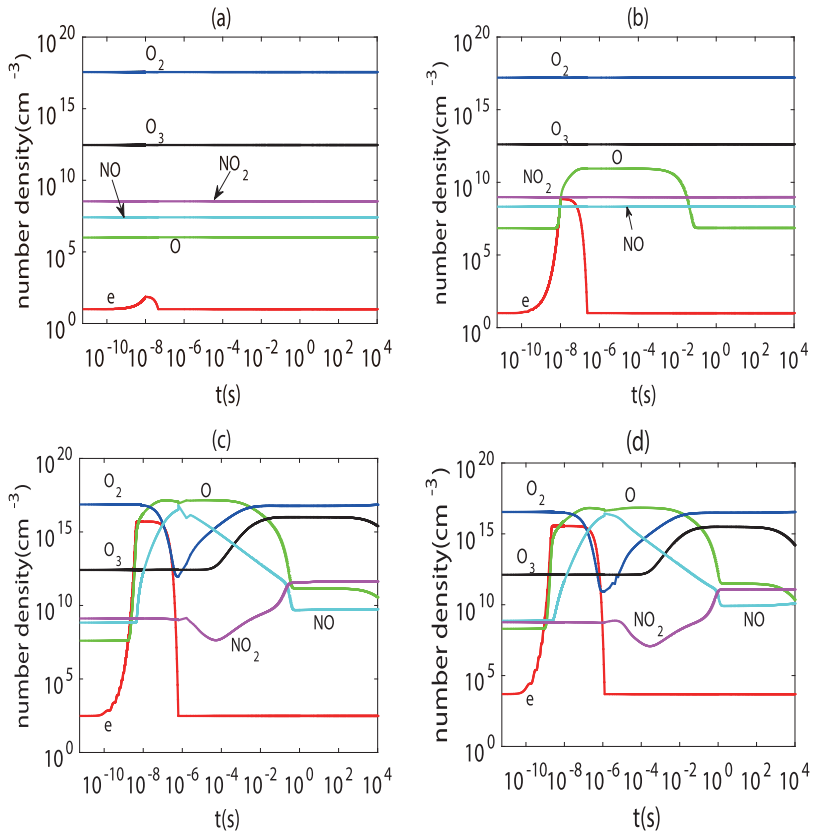

FIG. 6. Change of the plasma numbers over time under the action of single pulse at different heights: (a) 20 km; (b) 25 km; (c) 30 km; (d) 35 km.

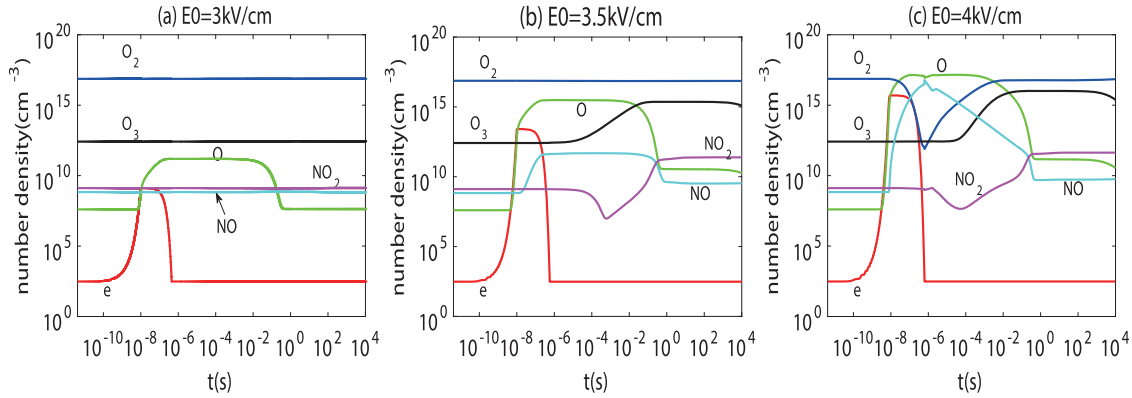

FIG. 7. Changes of the plasma particle numbers over time at 30km under the different electric field strength: (a) Ee=3 kV/cm; (b) Ee=3.5 kV/cm; (c) Ee=4.0 kV/cm.

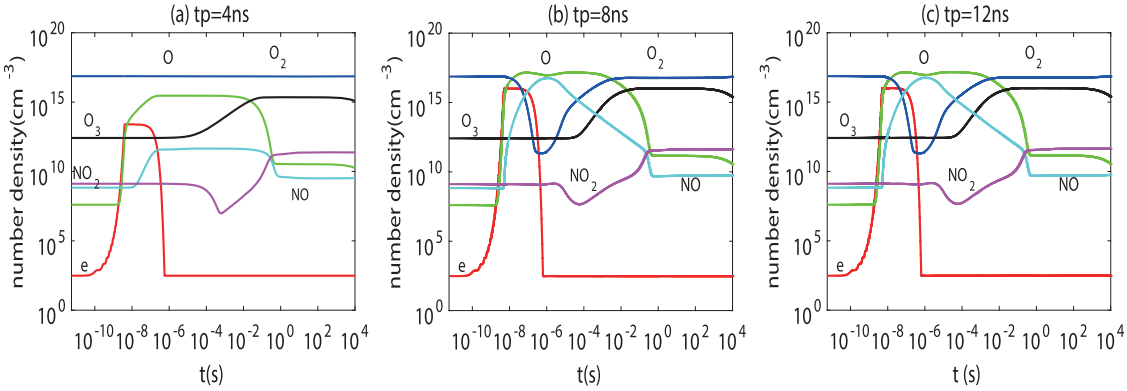

FIG. 8. Changes of the plasma particle numbers over time at 30km under the different pulse width: (a) tp=4 ns; (b) tp=8 ns; (c) tp=12 ns.

and tp=10ns under different field strength at 30 km. Figure 8 presents the results of f=3 GHz and Ee=4.8kV/cm^{-1} under different pulse width at 30 km.

The [O_3] has little change in Figure 7a but in Figure 7b~7c it has increased 2.3×10^{15} cm^{-3}, 1.02×10^{16} cm^{-3}. For Figure 8a~8c, the increase of [O_3] is 2.5×10^{15}cm^{-3}, 1.02×10^{16} cm^{-3} and 1.02×10^{16} cm^{-3}, respectively. Compare Figure 7 and Figure 8 to Figure 6c, the increase of field intensity and pulse width will benefit the occurrence of air breakdown and lead to an increase of electron density, it can be seen that when field intensity and pulse width is small, the electron density will be small, and the increase of [O_3] is not significant. Conversely, while the field intensity and pulse width is big enough, [O_3] will increase considerably.

As discussed above, it can be concluded that under the influence of HPM, considerable increase in electron number density will facilitate the conversion of O_2 to O_3. Besides, the increase of electron density can be achieved by increasing the microwave filed intensity or pulse width. It should be noted that this study has not consider gas diffusion, transport and other processes, consequently the simulation is confined to a small confined space. In the real atmosphere, O_3 will spread to other regions so that the density here may not grow such sharply like the above figures show.

V. CONCLUSIONS

In conclusion, high power microwave injection into the atmosphere provide a feasible method to maintain ozone balance. Simulation results illustrate that the electron density increases exponentially with time under the injection of HPM, reaching a maximum value of 10^{17}cm^{-3}, and at which time the electron temperature is high and the decomposition efficiency of CFCs is low. After the single pulse, the electron density begins to decay, the electron temperature decreases, and the decomposition efficiency becomes higher. Meanwhile, with the increase of field intensity, frequency and height, the decomposition efficiency of CFCs will increase. The decomposition rate of CFCs under single pulse can reach 6% according to the simulation result. The generation of a large number of free electrons in the ozone layer can promote the transformation of O_2 to O_3 and lead to a considerable increase in the ozone number density for a prolonged time. This paper simulates the change of the number density of several ozone layers (20 km, 25 km, 30 km, 35 km), and the simulation results was quantitatively analyzed. The results show that at the heights of 30 km and 35 km, the O_3 number density increases by at least three orders of magnitude compared to the initial number density and can maintain for about 400 seconds. By comparing the electron density curves, the generation mechanism of high power microwaves in the stratospheric O_3 was also analyzed.

Moreover, it should be pointed out that due to the simplification of the microwave propagation model, without considering the problems of diffusion, transport and other processes, the simulation is confined to a small confined space, the decomposition rate of CFCs may be relatively high than the actual value and O_3 will spread to other regions so that the density here may not grow sharply like the figures show. The next step will be ground simulation or space experiments to refine existing models and validate them.

ACKNOWLEDGMENTS

This work was supported by National Natural Science Foundation of China (NSFC Grants 41375007).

REFERENCES

[1]R. A. Akhmedzhanov, A. L. Vikharev, A. M. Gorbachev, O. A. Ivanov, N. G. Kolganov, A. L. Kolisko *et al.*, "Nanosecond microwave discharge as an ozone source in the upper atmosphere," Physics Letters A **207**(3–4), 209–213 (1995).

[2]R. A. Akhmedzhanov, A. L. Vikharev, A. M. Gorbachev, O. A. Ivanov, and A. L. Kolysko, "Investigation of the ozone formation process in a nanosecond microwave discharge in air and oxygen," Technical Physics **42**(3), 260–268 (1997).

[3]G. A. Askaryan, G. M. Batanov, A. E. Barkhudarov, S. I. Gritsinin, E. G. Korchagina, I. A. Kossyi *et al.*, "Electron attachment explodes freon molecules: new possibilities for removing freons from the atmosphere," JETP Letters **55**(9), 500 (1992).

[4]G. A. Askaryan, G. M. Batanov, A. E. Barkhudarov, S. I. Gritsinin, E. G. Korchagina, I. A. Kossyi *et al.*, "A freely localized microwave discharge for removal of chlorofluorocarbon contamination from the atmosphere," Journal of Physics D Applied Physics **27**(6), 1311–1318 (1994).
[5]G. M. Batanov, I. A. Kossyi, and V. P. Silakov, "Gas-discharge method for improving the environmental characteristics of the atmosphere (in memory of g.a. Askaryan)," Plasma Physics Reports **28**(3), 204–228 (2002).
[6]N. D. Borisov, S. I. Kozlov, and N. V. Smirnova, "Changes in the chemical composition of the middle atmosphere due to a multiple pulsed microwave discharge in air," Kosmicheskie Issledovaniia **31**(2), 63–74 (1993).
[7]G. P. Brasseur and S. Solomon, *Aeronomy of the Middle Atmosphere* (Springer Netherlands, 2005).
[8]J. K. Cao, D. F. Zhou, Z. X. Niu, Y. Shao, W. Zou, and Z. W. Xing, "Air breakdown by repetition-rate high power microwave pulse," High Power Laser & Particle Beams **18**(1), 115–118 (2006).
[9]B. Eliasson, U. Kogelschatz, and P. Baessler, "Dissociation of O_2 in N_2/O_2 mixtures," Journal of Physics B: Atomic and Molecular Physics **17**(22), L797–L801 (1984).
[10]D. B. Ge and Y. B. Yan, *Finite-Difference Time-Domain Method for Electromagnetic Waves (in Chinese)*, Xi'an: Xidian University Press, 2005.
[11]A. V. Gurevich, "An ionized layer in a gas (in the atmosphere)," Soviet Physics Uspekhi **132**(12), 685–690 (1980).
[12]A. V. Gurevich, *Non-linear phenomena in the ionosphere (in Chinese)*, Beijing: Science Press, 1986, P21–42.
[13]A. V. Gurevich, N. D. Borisov, N. A. Lukina, K. F. Sergeichev, I. A. Sychov, S. I. Kozlov *et al.*, "Intense growth of ozone concentration in subcritical fields in oxygen plasma," Physics Letters A **201**(2–3), 234–238 (1995).
[14]A. V. Gurevich, A. G. Litvak, A. L. Vikharev, O. A. Ivanov, N. D. Borisov, and K. F. Sergeichev, "Artificially ionized region as a source of ozone in the stratosphere," Physics–Uspekhi **43**(11), 1181–1202 (2000).
[15]G. J. M. Hagelaar and L. C. Pitchford, "Solving the Boltzmann equation to obtain electron transport coefficients and rate coefficients for fluid models," Plasma Sources Science and Technology **14**(4), 722 (2005).
[16]J. Heicklen, *Atmospheric Chemistry (in Chinese)* (Hunan Science and Technology Press, Changsha, 1981), pp. 10–11.
[17]T. Hu, D. F. Zhou, Q. R. Li, and Z. X. Niu, "Effect of electronic relaxation process on air breakdown caused by repetition frequency HPM," High Power Laser and Particle Beam **21**(4), 545–549 (2009).
[18]H. C. Kang, "Decomposition of chlorofluorocarbon by non-thermal plasma," J. Ind. Eng. Chem. **8**, 488 (2002).
[19]B. A. Klumov, "Destruction of the ozone layer as a result of a meteoroid falling into the ocean," JETP Letters **70**(5), 363–370 (1999).
[20]B. A. Klumov, "The creation of ozone holes as a consequence of meteoroids falls into the ocean," Advances in Space Research **28**(8), 1159–1167 (2001).
[21]Y. A. Lebedev, "Microwave discharges at low pressures and peculiarities of the processes in strongly non-uniform plasma," Plasma Sources Science and Technology **24**(5), 053001 (2015).
[22]A. D. Macdonald 1966, *Microwave breakdown in gases*, John Wiley & sons, New York.
[23]R. Morent and C. Leys, "Ozone generation in air by a dc-excited multi-pin-to-plane plasma source," Ozone Science & Engineering **27**(3), 239–245 (2005).
[24]J. M. Ouyang, *Study of atmospheric chemical processes in plasma radio* (National University of Defense Technology, Changsha, 2004).
[25]J. M. Ouyang, F. Q. Shao, and M. D. Lin, "Numerical simulation of ozone generation in oxygenic plasmas," Acta Physica Sinica **57**(5), 3293–3297 (2008).
[26]Y. P. Raizer and J. E. Allen, *Gas discharge physics* (Springer, Berlin, 1997).
[27]C. L. Ricketts, A. E. Wallis, J. C. Whitehead, and K. Zhang, "A mechanism for the destruction of CFC-12 in a nonthermal, atmospheric pressure plasma," Journal of Physical Chemistry A **108**(40), 8341–8345 (2004).
[28]Y. Y. Ruzhin, N. D. Borisov, and I. P. Nesterov, "Artificial beam injection in the stratosphere for modifying ozone depleted hazardous environment," A Model Approach. **2**(2), 1–7 (2015).
[29]T. H. Stix, "Removal of chlorofluorocarbons from the earth's atmosphere," Journal of Applied Physics **66**(11), 5622–5626 (1989).
[30]T. Tang, C. Liao, and D. Yang, "Feasibility of solving high-power microwave propagation in the atmosphere using FDTD method," Chinese Journal of Radio Science **25**(1), 122–126 (2010).
[31]T. Tang, C. Liao, Q. Gao, and P. Zhao, "Analysis of reflection properties of high power microwave propagation in mixture-atmosphere," Journal of Electromagnetic Analysis & Applications **2**, 543–548 (2010).
[32]T. Tang, *Numerical Investigation on the nonlinear problems of HPM pulses propagation through the atmosphere* (School of Physical Science and Technology of Southwest Jiaotong University, Chengdu, 2011).
[33]K. T. Tsang, D. M. Ho, R. J. Siverson, and A. Y. Wong 1991, "Stratospheric ozone conservation by electron attachment," *IEEE International Conference on Plasma Science, 1991. IEEE Conference Record–Abstracts* (pp. 182–183). IEEE.
[34]A. Vikharev, A. Gorbachev, O. Ivanov, A. Kolisko, and A. Litvak, "Modeling of the creation and kinetics of the artificial ionized layer in the upper atmosphere," Journal of Geophysical Research Atmospheres **99**(D10), 21097–21108 (1994).
[35]A. E. Wallis, J. C. Whitehead, and K. Zhang, "Plasma-assisted catalysis for the destruction of cfc-12 in atmospheric pressure gas streams using TiO2," Catalysis Letters **113**(1-2), 29–33 (2007).
[36]A. Y. Wong, J. Steinhauer, R. Close, T. Fukuchi, and G. M. Milikh, "Conservation of ozone in the upper atmosphere by selective ion removal," Comments on Plasma Physics & Controlled Fusion **12**, 223–234 (1989).
[37]N. L. Xiong, C. C. Tang, and X. J. Li, *Physical Introduction to Ionosphere* (Wuhan University Press, Wuhan, 1999), pp. P311–353.
[38]K. S. Yee, "Numerical solution of initial boundary value problems involving Maxwell's equations in isotropic media," IEEE Transactions on Antennas & Propagation **14**(3), 302–307 (1966).
[39]Z. C. Yuan and J. M. Shi, "Theoretical and numerical studies on interactions between high-power microwave and plasma," Acta Physica Sinica **63**(9), 3459–3467 (2014).
[40]P. C. Zhao, C. Liao, W. B. Lin, and T. Tao, "Numerical analyses of air ionization and breakdown of short-pulse high-power microwave," Journal of Southwest Jiaotong University **46**(1), 109–114 (2011).
[41]P. C. Zhao, C. Liao, T. Tang, and Q. M. Gao, "Fdtd calculation of high power microwave level propagation in air and breakdown analysis," Journal of Chongqing University of Posts & Telecommunications, Natural Science Edition (in Chinese) **22**(4), 431–435 (2010).
[42]Q. H. Zhou, Z. W. Dong, and J. Y. Chen, "Modeling of plasma pattern formation in 110 GHz microwave air breakdown," Acta Physica Sinica **60**(12), 125202 (2011).